

Crystal Structures and Topochemical Polymerizations of 7,7,8,8-Tetrakis(alkoxycarbonyl)quinodimethanes

Shinji Nomura,[†] Takahito Itoh,^{*,†} Hirofumi Nakasho,[†] Takahiro Uno,[†] Masataka Kubo,[†] Kazuki Sada,[‡] Katsunari Inoue,[§] and Mikiji Miyata[§]

Contribution from the Department of Chemistry for Materials, Faculty of Engineering, Mie University, 1515 Kamihama-cho, Tsu-shi, Mie 514-8507, Japan, Department of Chemistry and Biochemistry, Graduate School of Engineering, Kyushu University, 6-10-1 Hakozaki, Higashi-ku, Fukuoka 630-8528, Japan, and Department of Material and Life Science, Graduate School of Engineering, Osaka University and Handai FRC, 2-1 Yamadaoka, Suita, Osaka 565-0871, Japan

Received September 19, 2003; E-mail: itoh@chem.mie-u.ac.jp.

Abstract: Highly conjugated monomers, 7,7,8,8-tetrakis(alkoxycarbonyl)quinodimethanes (methoxy (**1a**), ethoxy (**1b**), isopropoxy (**1c**), benzyloxy (**1d**), chloroethoxy (**1e**), and bromoethoxy (**1f**)), were synthesized. Recrystallizations of **1a**, **1c**, **1e**, and **1f** yielded two crystal forms (prisms (**1a-A**) and needles (**1a-B**), needles (**1c-A**) and plates (**1c-B**), prisms (**1e-A**) and plates (**1e-B**), and prisms (**1f-A**) and needles (**1f-B**)), which have different molecular packing modes by X-ray crystal structure analysis, indicating that the crystals are polymorphic. In the photopolymerizations of these monomer crystals in the solid state, **1a-A**, **1e-A**, and **1f-A** polymerized topochemically to give crystalline polymers. For their thermal polymerizations in the solid state, in addition to **1a-A**, **1e-A**, and **1f-A**, **1e-B** and **1f-B** polymerized, but polymers formed from the **1e-B** and **1f-B** were amorphous. The packing of quinodimethane molecules in the crystals was defined by four kinds of parameters, stacking distance (d_s), the distance between the reacting exomethylene carbon atoms (d_{cc}), the angles formed between the stacking axis and longer axis of the monomer molecule (θ_1), and the shorter axis of the monomer molecule (θ_2), and then the polymerization reactivity of these quinodimethanes in the solid state was discussed on the basis of these parameters.

Introduction

Since primary structures of polymers such as stereoregularity, regioselectivity, molecular weight, molecular weight distribution, chain-end structures, and branching greatly influence physical properties, their control has been attracting much attention in polymer chemistry. Recent advances in "living polymerization" and "stereospecific polymerization" enable one to control primary structures precisely. Stereoregularity and regioselectivity have been achieved in the presence of catalysts, which has interaction with monomer or growing chain-end in solutions.¹ Another approach to control polymer structures is utility of regularity of monomer arrangements in the crystalline state because positions and orientations of the monomers do not change and motion of monomer is strongly limited. When the polymerization progresses without moving the center of gravity of the monomer in the crystal state, stereoregularity and regioselectivity ought to be controlled automatically. They are called as topochemical polymerizations. Despite high reactivities, stereoregularity, and regioselectivity, a limited number of monomers such as 2,5-distyrylpyridine derivatives and related

compounds,² diacetylene derivatives,³ triene and triacetylene derivatives,⁴ and muconic acid and sorbic acid derivatives⁵ have

- (2) (a) Hasegawa, M. *Chem. Rev.* **1983**, *83*, 507–518. (b) Hasegawa, M. *Adv. Phys. Org. Chem.* **1995**, *30*, 117–171.
- (3) (a) Wegner, G. Z. *Naturforsch. B* **1969**, *24*, 824–832. (b) Wenger, G. *Pure Appl. Chem.* **1977**, *49*, 443–454. (c) Enkelmann, V. *Adv. Polym. Sci.* **1984**, *63*, 91–131. (d) Ogawa, T. *Prog. Polym. Sci.* **1995**, *20*, 943–985. (e) Huntsman W. D. In *The Chemistry of Functional Groups. Supplement C: The Chemistry of Triple-Bonded Functional Groups*; Patai, S., Rappoport, Z., Eds.; John Wiley & Sons: New York, 1983; Chapter 22. (f) Okada, S.; Matsuda, H.; Nakanishi, H. In *Polymeric Materials Encyclopedia*; Salamone, J. C., Ed.; CRC Press: Boca Raton, 1996; pp 8393–8398. (g) Bloor, D.; Chance, R. R. *Polydiacetylenes*; NATO ASI Series E, Applied Sciences No. 102.; Martinus Nijhoff: Dordrecht, 1985.
- (4) (a) Kiji, J.; Kaiser, J.; Wegner, J. G.; Schulz, R. C. *Polymer* **1973**, *14*, 433–439. (b) Enkelmann, V. *Chem. Mater.* **1994**, *6*, 1337–1340. (c) Xiao, J.; Yang, M.; Lauher, J. W.; Fowler, F. W. *Angew. Chem., Int. Ed.* **2000**, *39*, 2132–2135. (d) Hoang, T.; Lauher, J. W.; Fowler, F. W. *J. Am. Chem. Soc.* **2002**, *124*, 10656–10657.
- (5) (a) Matsumoto, A.; Matsumura, T.; Aoki, S. *Macromolecules* **1996**, *29*, 423–432. (b) Matsumoto, A.; Yokoi, K.; Aoki, S.; Tashiro, K.; Kamae, T.; Kobayashi, M. *Macromolecules* **1998**, *31*, 2129–2136. (c) Matsumoto, A.; Odani, T.; Chikada, M.; Sada, K.; Miyata, M. *J. Am. Chem. Soc.* **1999**, *121*, 11122–11129. (d) Matsumoto, A.; Nagahama, S.; Odani, T. *J. Am. Chem. Soc.* **2000**, *122*, 9109–9119. (e) Odani, T.; Matsumoto, A. *Macromol. Rapid Commun.* **2000**, *21*, 40–44. (f) Matsumoto, A.; Katayama, K.; Odani, T.; Oka, K.; Tashiro, K.; Saragai, S.; Nakamoto, S. *Macromolecules* **2000**, *33*, 7786–7792. (g) Nagahama, S.; Matsumoto, A. *J. Am. Chem. Soc.* **2001**, *123*, 12176–12181. (h) Matsumoto, A.; Odani, T. *Macromol. Rapid Commun.* **2001**, *22*, 1195–1215. (i) Matsumoto, A.; Sada, K.; Tashiro, K.; Miyata, M.; Tsubouchi, T.; Tanaka, T.; Odani, T.; Nagahama, S.; Tanaka, T.; Inoue, K.; Saragai, S.; Nakamoto, S. *Angew. Chem., Int. Ed.* **2002**, *41*, 2502–2505. (j) Matsumoto, A.; Tanaka, T.; Tsubouchi, T.; Tashiro, K.; Saragai, S.; Nakamoto, S. *J. Am. Chem. Soc.* **2002**, *124*, 8891–8902. (k) Tanaka, T.; Matsumoto, A. *J. Am. Chem. Soc.* **2002**, *124*, 9676–9677.

* Corresponding author. Phone: +81-59-231-9410. Fax: +81-59-231-9410.

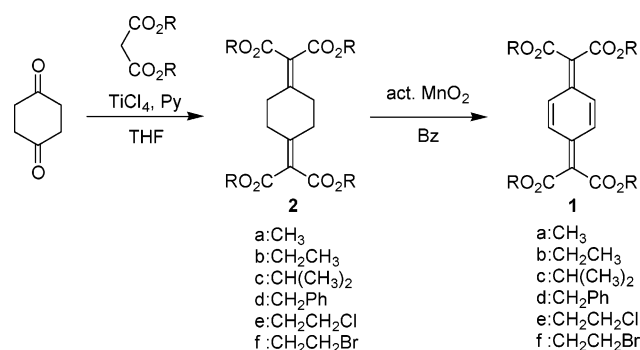
[†] Mie University.

[‡] Kyushu University.

[§] Osaka University and Handai FRC.

(1) Okamoto, Y.; Nakano, T. *Chem. Rev.* **1994**, *94*, 349–372.

Scheme 1



been reported to undergo topochemical polymerizations, because they have strict requirement of the monomer arrangements in crystalline state. Recently, we reported as a preliminary result that a conjugated monomer, 7,7,8,8-tetrakis(methoxycarbonyl)quinodimethane (**1a**), gave two crystal forms (prisms and needles) and exhibited drastic differences in the polymerization ability observed between them. That is, the prisms polymerized topochemically but the needles did not, arising from the difference in the packing modes.⁶ Here, to establish general rules in the topochemical polymerizations, it is worthwhile to clarify the relation between crystal structures of quinodimethane monomers and their solid-state polymerization reactivities by using various quinodimethane monomers. In this work, we describe the syntheses of 7,7,8,8-tetrakis(alkoxycarbonyl)quinodimethanes bearing various alkoxy groups and determination of their crystal structures by X-ray crystal analysis and also discuss the relationship of the solid-state polymerization reactivity with the packing in the crystals.

Results and Discussion

Monomer Synthesis and Recrystallization. Monomers (**1a–f**) were synthesized by a synthetic route as shown in Scheme 1. Knoevenagel condensations of 1,4-cyclohexanedione and corresponding dialkyl malonates using titanium tetrachloride and pyridine as a dehydrating reagent⁷ afforded 1,4-[bis(alkoxycarbonyl)methylene]cyclohexanes (**2a–f**) (42–68% yields). Oxidation of **2a–f** with activated manganese dioxide in refluxing benzene gave 7,7,8,8-tetrakis(alkoxycarbonyl)quinodimethanes (**1a–f**) (16–37% yields). All monomers were identified by ¹H and ¹³C NMR and IR spectroscopies and elemental analysis.

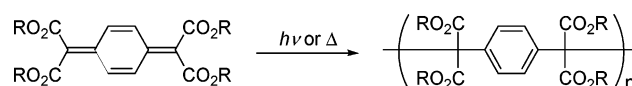
Those monomers were recrystallized from various conditions to obtain fine crystals for polymerization and single crystals suitable for X-ray crystallography. Recrystallizations of **1a**, **1c**, **1e**, and **1f** from hexane gave a mixture of two crystal forms, yellow prisms (**1a–A**) and yellow needles (**1a–B**) for **1a**, yellow needles (**1c–A**) and pale yellow plates (**1c–B**) for **1c**, yellow prisms (**1e–A**) and pale yellow plates (**1e–B**) for **1e**, and yellow prisms (**1f–A**) and yellow needles (**1f–B**) for **1f**, indicating that they have polymorphism. After many trials of screening of recrystallization conditions such as solvents, concentrations, and temperature, we found the conditions that gave one of two polymorphs exclusively for **1a**, **1c**, **1e**, and **1f**; **1a–A** from chloroform/hexane (1/3 v/v) and **1a–B** from methanol, **1c–A** from hexane at high concentration (250 mg/40 mL) and **1c–B** at low concentration (160 mg/40 mL), **1e–A** from

Table 1. Photopolymerizations of **1a–f** in the Solid State

run	monomer	crystal	temp. (°C)	time (h)	form	conv. (%)	<i>M_n</i>
1	1a–A		30	3	off-white prism	>99	ND ^a
2	1a–B		30	6		0	
3	1b		30	24		0	
4	1c–A		30	24		0	
5	1c–B		30	24		0	
6	1d		30	24		0	
7	1e–A		30	3	ivory prism	>99	ND ^a
8	1e–B		30	24		0	
9	1f–A		30	0.5	orange plate	>99	ND ^a
10	1f–B		30	24		0	

^a Not determined (insoluble in common organic solvents).

Scheme 2



chloroform/hexane (2/3 v/v) and **1e–B** from chloroform/hexane (3/2 v/v), and **1f–A** from chloroform and **1f–B** from chloroform/hexane (1/2 v/v). Both **1b** and **1d** gave only one crystal form (yellow needles) under the all attempted recrystallization conditions.

Solid-State Polymerization. Monomer crystals were each subjected to polymerization by irradiation using a high-pressure Hg lamp at 30 °C, and the results are summarized in Table 1. **1a–A**, **1e–A**, and **1f–A** polymerized to give the corresponding polymers as crystal-like solids, which were insoluble in common organic solvents such as chloroform, benzene, tetrahydrofuran (THF), dimethyl sulfoxide, *N,N*-dimethylformamide, methanol, and hexane. While no polymerizations occurred for **1a–B**, **1b**, **1c–A**, **1c–B**, **1d**, **1e–B**, and **1f–B**, and unreacted monomers were recovered quantitatively. The resulting polymers of **1a–A**, **1e–A**, and **1f–A** were only characterized by IR spectroscopy and elemental analysis because of their insolubilities in these organic solvents. In the IR spectra of polymers from **1a–A**, **1e–A**, and **1f–A**, characteristic absorption bands at 1533–1546 cm⁻¹ assigned to the exocyclic conjugated carbon–carbon double bond of the quinodimethane monomers disappeared, and the new bands arising from carbon–carbon double bonds of the aromatic ring were observed at ca. 1500, 1400 cm⁻¹, and a band arising from out-of-plane deformation of the *para*-substituted benzene, characteristic of a two-adjacent-hydrogen system, was observed at ca. 800 cm⁻¹. These spectrum changes observed in the solid-state polymerizations of **1a–A**, **1e–A**, and **1f–A** strongly support that polymerization reactions of substituted quinodimethane molecules take place at the disubstituted exomethylene carbon atoms with the formation of the corresponding stable aromatic structures.⁸ Moreover, elemental analysis values of the products were in good agreement with the calculated ones for the corresponding polymers. Therefore, the photopolymerizations in the crystalline state proceed in the same manner as those in the conventional polymerizations in solution, as shown in Scheme 2.

On the other hand, we tried thermal polymerizations of these monomer crystals by heating in the dark at a temperature 10 °C lower than each melting point, and the results are summarized

- (8) (a) Iwatsuki, S.; Itoh, T. *Macromolecules* **1980**, *13*, 983–989. (b) Iwatsuki, S.; Itoh, T.; Yokotani, I. *Macromolecules* **1983**, *16*, 1817–1823. (c) Iwatsuki, S.; Itoh, T.; Iwai, T.; Sawada, H. *Macromolecules* **1985**, *18*, 2726–2732. (d) Itoh, T.; Okano, H.; Hishida, T.; Inokuchi, A.; Kamei, N.; Sato, T.; Kubo, M.; Iwatsuki, S. *Tetrahedron* **1997**, *53*, 15247–15261. (e) Itoh, T.; Iwatsuki, S. *Macromol. Chem. Phys.* **1997**, *198*, 1997–2016. (f) Itoh, T. *Prog. Polym. Sci.* **2001**, *26*, 1019–1059.

(6) Itoh, T.; Nomura, S.; Uno, T.; Kubo, M.; Sada, K.; Miyata, M. *Angew. Chem., Int. Ed.* **2002**, *41*, 4306–4309.

(7) Lehnert, W. *Tetrahedron* **1973**, *29*, 635–638.

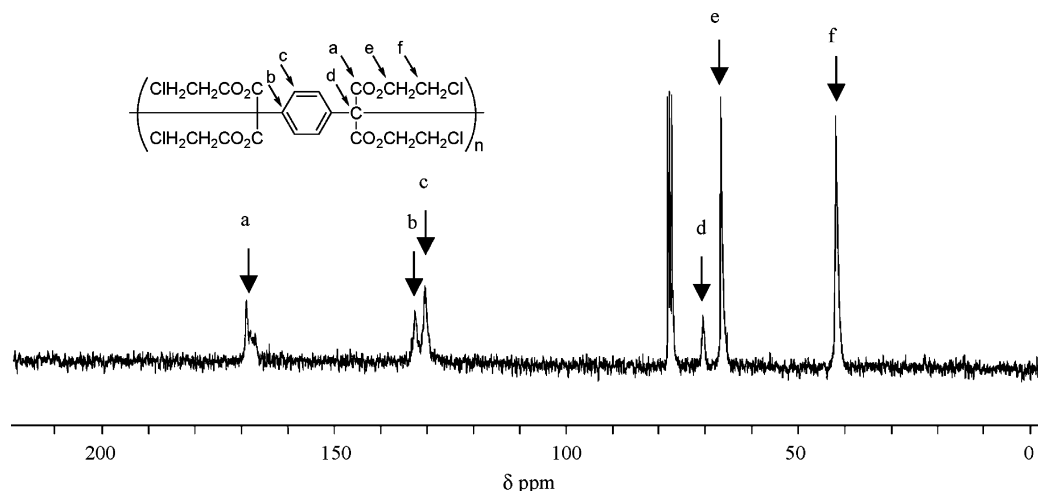


Figure 1. ^{13}C NMR spectrum in chloroform-*d* of the polymer of **1e-B** obtained by solid-state thermal polymerization.

Table 2. Thermal Polymerizations of **1a-f** in the Solid State

run	monomer	crystal	temp. (°C)	time (h)	form	conv. (%)	M_n
11	1a-A		60	3	off-white prism	47	ND ^a
12	1a-B		60	6		0	
13	1b		60	24		0	
14	1c-A		100	24		0	
15	1c-B		90	24		0	
16	1d		60	24		0	
17	1e-A		90	24	ivory prism	72	ND ^a
18	1e-B		105	24	yellow solid	94	15000
19	1f-A		60	24	orange plate	46	ND ^a
20	1f-B		120	15	white solid	>99	ND ^a
21	1e^b		60	87	white powder	21	4100
22	1f^c		60	4 days	white powder	2	3400

^a Not determined (insoluble in common organic solvents). ^b Solution polymerization in toluene, 2.5 mL; **1e**, 372 mg; AIBN, 6.0 mg. ^c Solution polymerization in chloroform, 10 mL; **1f**, 400 mg; AIBN, 10 mg.

in Table 2. In addition to photopolymerizable **1a-A**, **1e-A**, and **1f-A**, **1e-B** and **1f-B** were found to be polymerized by heating. The polymer yields at the thermal polymerizations for **1a-A**, **1e-A**, and **1f-A** were lower than those at the photopolymerizations. Thermal polymerizations of **1e-B** at 105 °C and of **1f-B** at 120 °C gave the corresponding polymers as yellow solids and a white one, respectively. The polymers of **1a-A**, **1e-A**, and **1f-A** had the same solubilities as the polymers obtained by the photopolymerizations. On the other hand, the polymer of **1e-B** was soluble in chloroform, THF, and benzene but insoluble in methanol and hexane, and the polymer of **1f-B** was insoluble in common organic solvents such as chloroform, THF, benzene, methanol, and hexane. For all cases, solid-state thermal polymerization occurred; the IR spectra of the polymers had similar changes to those produced by photopolymerization. Here, the polymer of **1e-B** was further characterized by GPC and ^{13}C NMR spectroscopy because of its high solubility toward common organic solvents. The number-average molecular weight (M_n) was determined to be 15 000, and the ^{13}C NMR spectrum of the polymer of **1e-B** is shown in Figure 1, which was the same as that of the polymer obtained by solution polymerization described below, supporting the formation of the corresponding stable *para*-substituted benzene structure by radical coupling reactions between the exomethylene carbon atoms of the quinodimethane structure.

In this way, **1e-B** and **1f-B** showed different polymerization behavior, depending upon the polymerization conditions; they polymerized in the solid-state thermal polymerization conditions but not in the photopolymerization conditions. Probably, in

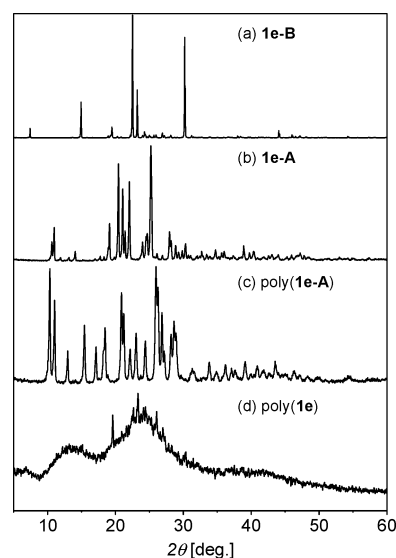


Figure 2. Powder XRD patterns of (a) **1e-B**, (b) **1e-A**, (c) polymer of **1e-A** obtained by photopolymerization, and (d) polymer of **1e** obtained by solution polymerization.

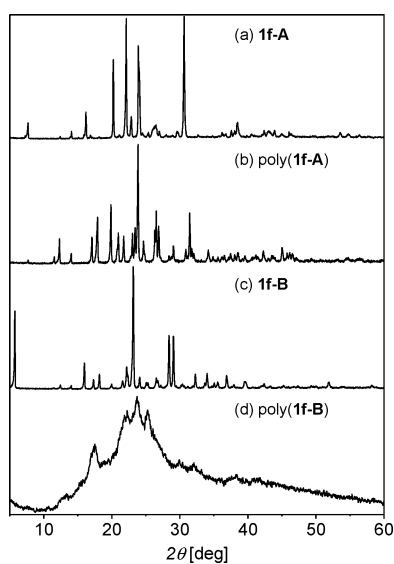
photopolymerization at temperatures as low as 30 °C, the motion of the molecules in the crystals is significantly limited, but at temperatures near each melting point, the molecules in the crystals would be allowed to move into reaction because of enhanced molecular motion. To compare the solid-state polymerization reactivity of **1e** and **1f**, their solution polymerizations with AIBN as an initiator were carried out, and the results (run 21 and 22) are shown in Table 2. The molecular weights and the polymer yields were lower in comparison with those in the solid-state polymerization.

Crystallinity of Obtained Polymers. Polymers of **1a-A**, **1e-A**, and **1f-A** obtained by photopolymerizations and solid-state thermal polymerizations and also the polymer of **1f-B** by solid-state thermal polymerization were insoluble in common organic solvents, and their shapes were similar to those of the corresponding monomers. Thus, the crystallinity of the obtained polymers was investigated by powder XRD. The powder XRD patterns of monomers **1e-A**, **1f-A**, and **1f-B** and the corresponding polymers are shown in Figures 2 and 3, respectively

Very sharp diffraction patterns of the polymers obtained by the photopolymerizations of **1e-A** and **1f-A** indicate that

Table 3. Crystallographic Data for Crystals of 7,7,8,8-Tetrakis(alkoxycarbonyl)quinodimethanes

monomer	1a-A	1a-B	1b	1c-A	1c-B	1d	1e-A	1e-B	1f-A	1f-B
formula	C ₁₆ H ₁₆ O ₈	C ₁₆ H ₁₆ O ₈	C ₂₀ H ₂₄ O ₈	C ₂₄ H ₃₂ O ₈	C ₂₄ H ₃₂ O ₈	C ₄₀ H ₃₂ O ₈	C ₂₀ H ₂₀ Cl ₄ O ₈	C ₂₀ H ₂₀ Cl ₄ O ₈	C ₂₀ H ₂₀ Br ₄ O ₈	C ₂₀ H ₂₀ Br ₄ O ₈
fw	336.29	336.29	392.40	448.51	448.51	640.68	530.19	530.19	707.99	707.99
crystal system	monoclinic	triclinic	orthorhombic	monoclinic	monoclinic	monoclinic	monoclinic	monoclinic	triclinic	monoclinic
space group	<i>P</i> 2 ₁ / <i>n</i> (#14)	<i>P</i> 1̄ (#2)	<i>I</i> ba2 (#45)	<i>C</i> 2/ <i>c</i> (#15)	<i>C</i> 2/ <i>c</i> (#15)	<i>P</i> 2 ₁ / <i>c</i> (#14)	<i>P</i> 2 ₁ / <i>c</i> (#14)	<i>P</i> 2 ₁ / <i>c</i> (#14)	<i>P</i> 1̄ (#2)	<i>P</i> 2 ₁ / <i>c</i> (#14)
<i>a</i> , Å	8.6787(7)	8.6023(4)	13.483(2)	24.60(1)	15.760(6)	10.8775(8)	7.6460(5)	11.934(3)	6.9884(8)	4.9861(5)
<i>b</i> , Å	7.5719(7)	8.889(2)	21.392(3)	9.724(1)	8.4013(8)	7.9949(3)	15.981(2)	7.640(1)	7.7551(6)	30.653(2)
<i>c</i> , Å	12.761(1)	5.2870(6)	6.8956(9)	10.864(2)	19.395(2)	18.0881(9)	10.006(1)	12.737(2)	12.177(1)	8.0969(5)
α , deg	90	96.305(4)	90	90	90	90	90	90	102.295(3)	90
β , deg	105.193(2)	105.636(5)	90	109.32(2)	99.29(2)	92.459(5)	105.371(4)	97.145(9)	97.575(3)	98.386(4)
γ , deg	90	87.323(8)	90	90	90	90	90	90	106.277(6)	90
<i>V</i> , Å ³	809.2(1)	386.87(9)	1988.9(5)	2452(1)	2534.27	1571.6(2)	1178.9(2)	1152.3(4)	605.92(10)	1224.3(2)
<i>Z</i>	2	1	4	4	4	2	2	2	1	2
ρ_{calc} , g/cm ³	1.380	1.443	1.310	1.215	1.175	1.354	1.493	1.528	1.940	1.920
unique reflcns	1828	1711	860	1774	1922	2652	2099	2034	2063	2167
no. obsd reflns	1477	1360	832	1679	1514	2276	1713	1749	1871	1490
<i>R</i> ₁	0.046	0.062	0.072	0.053	0.053	0.056	0.051	0.109	0.103	0.070
<i>R</i> , <i>R</i> _w	0.106, 0.133	0.131, 0.183	0.291, 0.156	0.083, 0.117	0.076, 0.091	0.116, 0.151	0.090, 0.133	0.253, 0.267	0.151, 0.357	0.109, 0.196
GOF	1.27	1.82	1.56	1.67	1.51	1.86	1.37	2.00	1.75	1.49
2 θ_{max} , deg	55.0	54.9	136.3	51.2	51.2	136.3	136.4	136.4	66.8	136.4
temp, °C	25	25	23	-76	-76	-69	23	23	-80	23

**Figure 3.** Powder XRD patterns of (a) **1f-A**, (b) polymer of **1f-A** obtained by photopolymerization, (c) **1f-B**, and (d) polymer of **1f-B** obtained by solid-state thermal polymerization.

1e-A and **1f-A** show no less crystallinity after completion of the polymerizations. Further, 2θ of diffraction peaks arising from crystalline polymers are in fairly good agreement with those of the respective monomers. In particular, the powder XRD pattern of polymer from the solid-state polymerization of **1e-A** is significantly different from that of polymer obtained from the solution polymerization (run 21 in Table 2) of **1e** in toluene initiated by AIBN (Figure 2). Therefore, these points indicate that the polymerizations of those crystals as well as **1a-A**⁶ proceed topochemically. On the other hand, the broad diffraction pattern of polymer from the solid-state thermal polymerization of **1f-B** indicates that **1f-B** shows loss of crystallinity during the polymerization (Figure 3). The crystalline polymers of **1e-A** and **1f-A** obtained by photopolymerization and thermal polymerization in the solid-state melted at 149–156 and 155–164 °C, respectively. After melting, the solubility of both polymers changed dramatically, and they became soluble in chloroform, THF, and benzene. Also, their ¹H NMR and ¹³C NMR spectra were the same as those of the polymers obtained by their solution polymerizations, and their molecular weights

were ca. 20 000. It is, therefore, considered that the insolubility in common organic solvents for both polymers of **1e-A** and **1f-A** obtained by solid-state polymerization is due to their high crystallinities and/or high molecular weights.

Crystal Structures and Polymerization Reactivity in the Crystalline State. To clarify the packing modes of the molecules in the crystals, we investigated the crystal structures by X-ray crystallography systematically. Measurements were carried out using the imaging plate diffractometer system, and during measurements polymerizations of monomer crystals did not take place. The crystallographic data of **1a-f** are summarized in Table 3, and their crystal structures are shown in Figure 4.

X-ray studies revealed differences of the crystal structures of two polymorphs of **1a**, **1c**, **1e**, and **1f**. In the latter three quinodimethanes, the polymorphisms are attributed to both the conformational difference of the ester groups and the crystal packings. Flexibilities of the alkyl chains and free rotation between exomethylene and carbonyl groups give variations of conformational isomerism. From the lattice parameters and the crystal structures, there are no apparent robust structural motifs in these compounds. However, the planar quinodimethane moieties tend to stack along one axis to form columnar structures as shown Figure 5.

The stacking manner in the columnar structure is affected by the alkyl groups of the esters. Moreover, association modes of the columns to 3D crystalline lattice are also changed by the ester groups. Therefore, the alkyl groups induce the change of monomer packing as well as polymerization reactivity in the crystalline state.

To discuss molecular arrangements of quinodimethanes in the crystal structures in relation to the solid-state polymerization reactivities, we investigated the stacking manners in the columnar structures by using structural parameters (d_s , d_{cc} , θ_1 , and θ_2). They are used by estimation of the stacking manner for diene monomers, because the quinodimethane monomers have planar structures similar to diene monomers.⁵ⁱ We examined these parameters defined as the angles formed between the stacking axis and longer axis of the monomer molecule (θ_1) and the shorter axis of the monomer molecule (θ_2), the distance between equivalent atoms in the stacked monomers (stacking distance, d_s), and the distance between the reacting exomethylene carbons

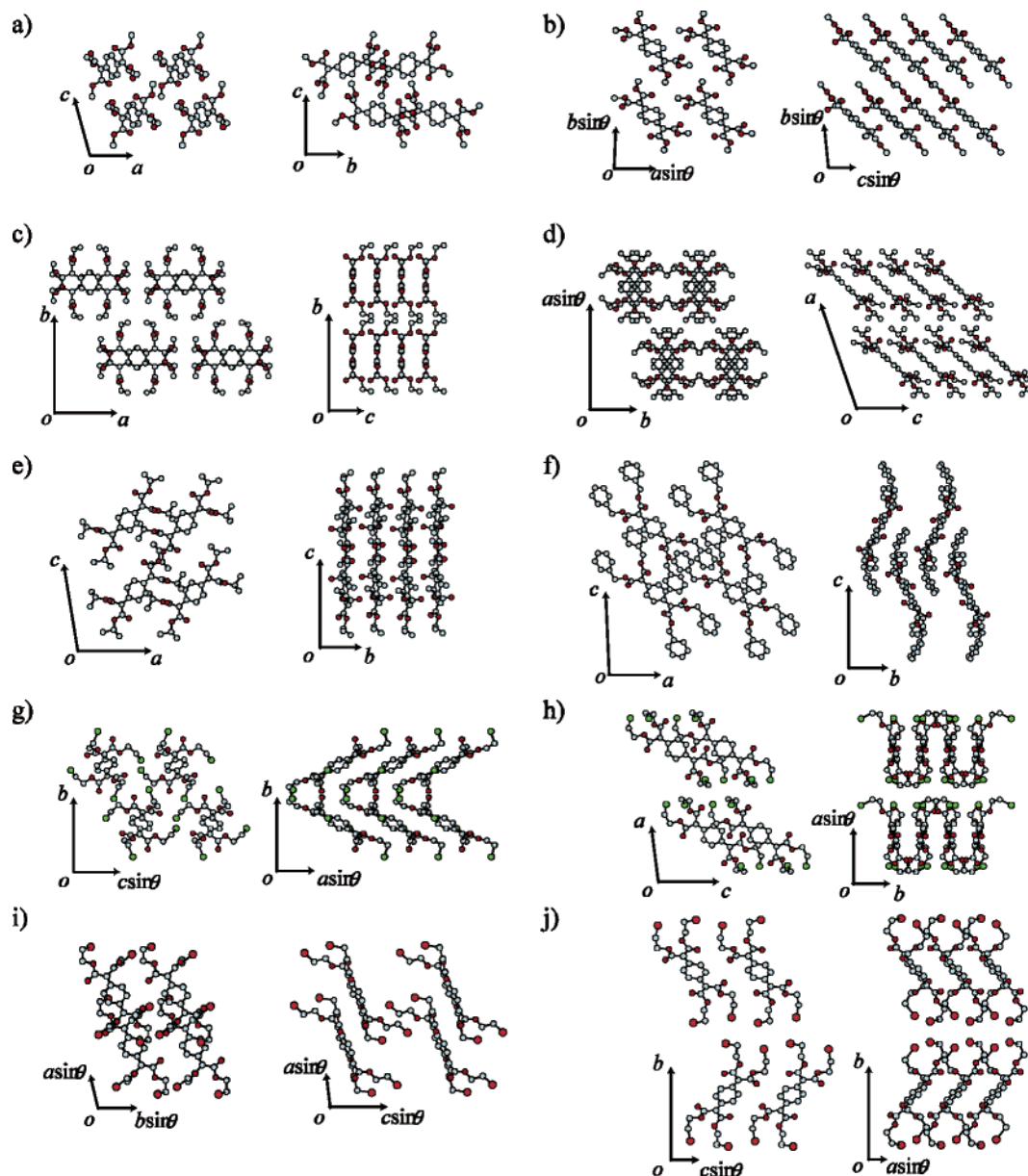


Figure 4. Crystal structures of the quinodimethane monomers: (a) **1a**–A, (b) **1a**–B, (c) **1b**, (d) **1c**–A, (e) **1c**–B, (f) **1d**, (g) **1e**–A, (h) **1e**–B, (i) **1f**–A, and (j) **1f**–B. Hydrogen atoms are omitted for clarity. Open and filled circles represent carbon and oxygen atoms, respectively.

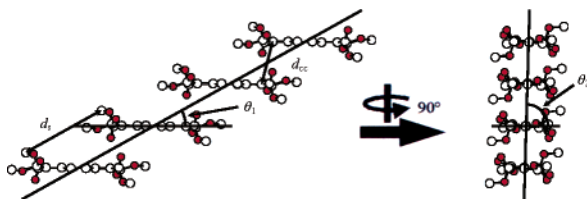


Figure 5. Stacking model for the quinodimethane monomers in the crystals, and the definition of stacking parameters for the prediction of the topochemical polymerization reactivity. d_s is the stacking distance between the adjacent monomers in a column; d_{cc} is the distance between the reacting exomethylene carbons; θ_1 and θ_2 are the angles between the stacking axis and longer axis of the monomer molecule and the shorter axis of the molecule.

(d_{cc}). The parameters of **1a**–**f** are summarized in Table 4, and the columns in the crystal structures are shown in Figure 6.

On the basis of stacking manners of the columnar structures, the crystal structures are divided into several groups: (i) the stacking axis is perpendicular to the molecular plane of the

Table 4. Stacking Parameters for Crystals of **1a**–**f**^a

monomer	θ_1 (deg)	θ_2 (deg)	d_s (Å)	d_{cc} (Å)
1a –A	30	89	7.6	3.9
1a –B	55	62	5.3	5.0
1b	90	90	3.4	4.3
1c –A	46	74	5.4	4.4
1c –B	49	41	8.9	6.8
1d	60	72	9.9	7.7
	43	47		
1e –A	32	83	7.6	4.2
1e –B	40	70	7.4	5.2
	50	52		
1f –A	33	89	7.0	3.8
1f –B	56	65	5.0	5.0

^a θ_1 , θ_2 , tilt angles of the molecular plane; d_{cc} , distance between the reacting exomethylene carbons; d_s , stacking distance.

quinodimethane, that is, both the tilt angles (θ_1 and θ_2) are 90° for **1b**, (ii) the stacking axis is tilted to the direction of the longer molecular axis ($\theta_1 \neq 90^\circ$) and not to that of the shorter

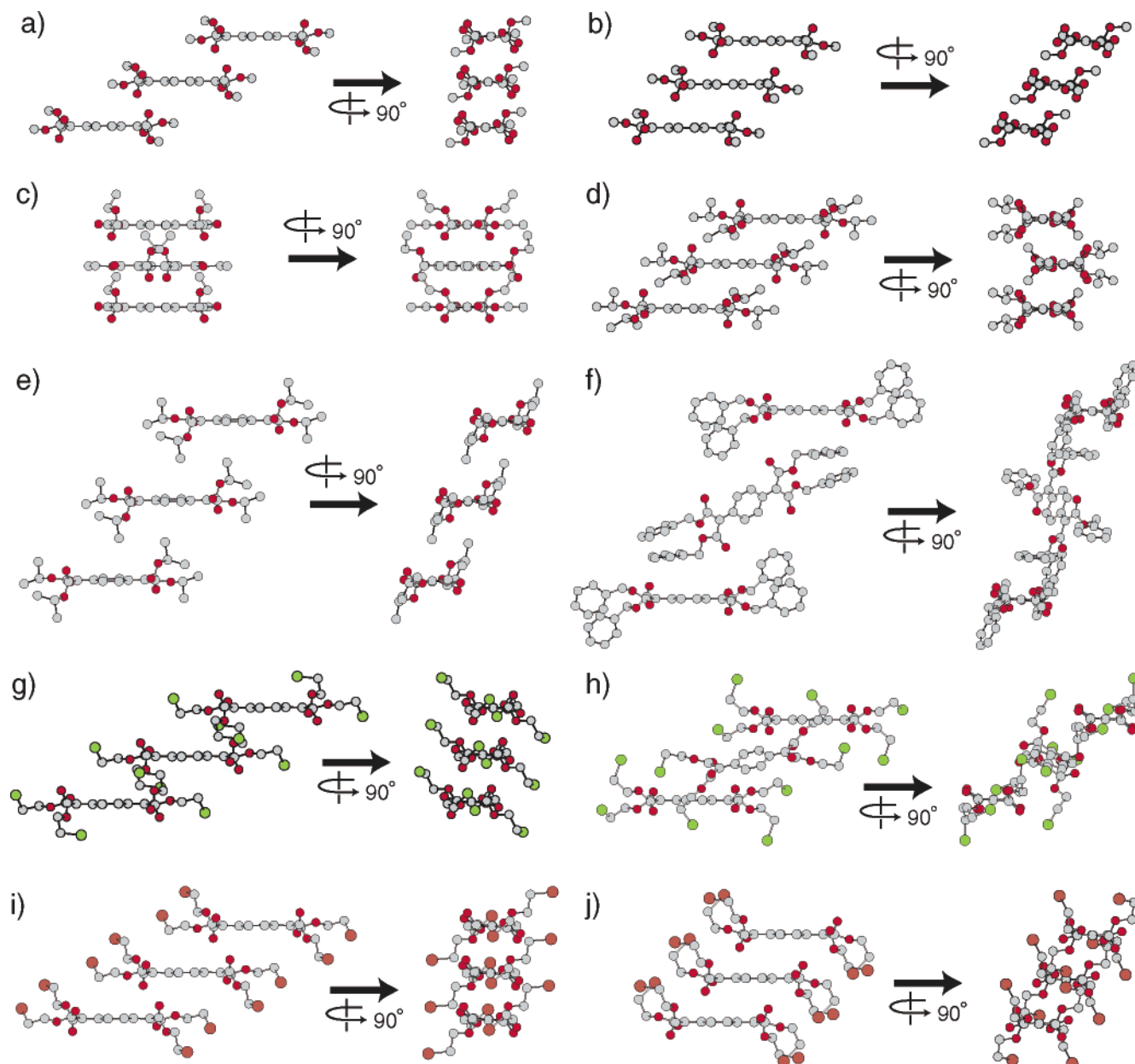


Figure 6. Columnar stackings of the quinodimethane monomers: (a) **1a-A**, (b) **1a-B**, (c) **1b**, (d) **1c-A**, (e) **1c-B**, (f) **1d**, (g) **1e-A**, (h) **1e-B**, (i) **1f-A**, and (j) **1f-B**. Hydrogen atoms are omitted for clarity. Open and filled circles represent carbon and oxygen atoms, respectively.

molecular axis ($\theta_2 = 90^\circ$) for **1a-A**, **1e-A**, and **1f-A**, and (iii) the stacking axis is tilted to an arbitrary direction ($\theta_1 \neq 90^\circ$, $\theta_2 \neq 90^\circ$) for **1a-B**, **1c-A**, **1c-B**, **1d**, **1e-B**, and **1f-B**. In the first type, the quinodimethane stacks exactly on the plane of the neighboring quinodimethane. The length between two quinodimethane planes, d_s , is 3.4 Å, which corresponds to the width of the quinodimethane and the length of π - π stacking. Steric repulsions between the ester moieties induce rotation of the quinodimethane plane along the stacking axis (60°). As a result, the distance between the reacting exomethylene carbon atoms, d_{cc} , is 4.3 Å and a little longer for polymerizations. In the second type, the stacking axis is inclined to the long molecular axis of the quinodimethane plane, and this produces offset stacking of the quinodimethanes. Then, the stacking distances are longer than the first type and the distances between the exomethylene carbons are shorter. No offsets to the shorter molecular axis get the reacting carbons close to each other.

Therefore, the stacking distances are in the small range of 7.0–7.6 Å, and d_{cc} s are 3.8–4.2 Å. In the last group, the stacking axes are tilted to arbitrary directions, which provides a wide range of stacking manners in the columns. The crystal structures of **1a-B**, **1c-B**, and **1f-B** have parallel stacking, similar to those of the first two types, and **1c-A** provides the similar parallel stacking but the quinodimethanes are arranged in a zigzag fashion. In the cases of **1d** and **1e-B**, the quinodimethane molecules are no longer parallel to the nearest neighbors. Therefore, the stacking distances are in the range of 7.4–9.9 Å and d_{cc} s are 5.2–7.7 Å.

On the other hand, monomers examined in this work could be classified into three groups by the difference in solid-state polymerization reactivities: (i) topochemical polymerizations by the photopolymerizations and the thermal polymerizations occurred to afford highly crystalline polymers for **1a-A**, **1e-A**, and **1f-A**, (ii) the thermal polymerizations occurred to give

amorphous polymers for **1e-B** and **1f-B**, and (iii) no polymerizations took place for **1a-B**, **1b**, **1c-A**, **1c-B**, and **1d**. All the topochemically polymerizable monomers (**1a-A**, **1e-A**, and **1f-A**) are in the second type of crystal structures with parameters of $\theta_1 = 30\text{--}33^\circ$, $\theta_2 = 83\text{--}89^\circ$, $d_s = 7.0\text{--}7.6 \text{ \AA}$, and $d_{cc} = 3.8\text{--}4.2 \text{ \AA}$. Nearly face-to-face stacking with some offset along the longer molecular axis is requisite for crystalline state polymerizations of quinodimethane monomers. When monomer molecules were stacked in this specific distance in the crystals, reacting exomethylene carbons can be brought close enough ($d_{cc} = 3.8\text{--}4.2 \text{ \AA}$) only by rotation of the monomer without movement of a translational direction. In particular, the d_s is quite similar to that of the repeating distance (about 7.3 \AA , calculated by molecular modeling) of the resulting polymer. This similarity of the unit lengths before and after polymerization affords high reactivities in the crystalline state and polymers with high crystallinity and molecular weight.

On the other hand, the d_s of the monomers in the groups ii and iii, except for **1e-B**, is much shorter or longer than 7.3 \AA . Longer d_s in **1c-B**, **1d**, and **1c-A** have d_{cc} values more than 4.2 \AA , and **1c-B** and **1d** have d_s values more than 8.5 \AA ; monomer molecules in crystals cannot move such a long distance and fail to polymerize. Most of them cannot polymerize in the crystalline state efficiently. From the above points, it is concluded that topochemical polymerization of quinodimethanes needs to have a d_{cc} value of about 4.0 \AA and translational arrangement of the monomers along the direction of polymerization, in addition to a d_s value of about 7.3 \AA , which is the fiber period of quinodimethane polymers. In the case of **1e-B**, polymerization occurred at high temperature, and the polymerization led to an amorphous polymer. This can be explained as follows. First, **1e-B** has a d_s value of 7.4 \AA and a d_{cc} value of 5.2 \AA , and the latter value is larger than the d_{cc} value of ca. 4.0 \AA suitable for topochemical polymerization. This means that monomer molecules have to move a long distance to polymerize. As a result, collapse of the crystals occurs and an amorphous polymer is produced. Second, there are two nearest-neighboring molecules because of the screw axis in the space group ($P2_1/c$), and therefore, there are two possible directions (path A and path B) for the polymerization reaction as shown in Figure 7, and the carbon-carbon bond formation between the reacting exomethylene carbons might occur at random, resulting in an amorphous polymer.

As another possibility, phase transition of the crystals, is plausible because a weak endothermic peak was observed at $102 \text{ }^\circ\text{C}$ for **1e-B** by DSC measurement, and details are now in progress.

The fiber period of quinodimethane polymers could be estimated to be about 7.3 \AA by molecular modeling. Therefore,

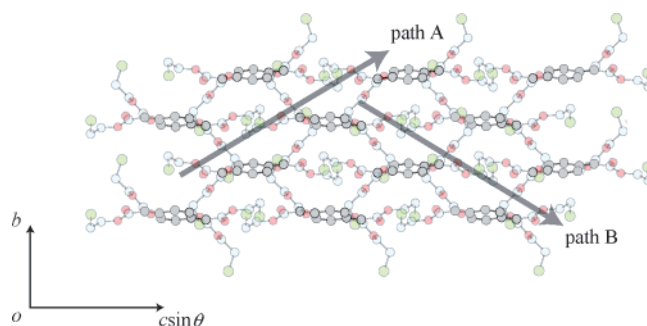


Figure 7. Packing mode of molecules in the crystals for **1e-B** and possible direction of polymerization.

if quinodimethane monomers have a d_s value of about 7.3 \AA in crystals, polymerization reactions would take place topochemically along the column axis. As the monomers in group i have d_s values of $7.0\text{--}7.6 \text{ \AA}$, close to the fiber period of about 7.3 \AA , topochemical polymerization could surely take place. For the monomers in group ii, as **1f-B** has a d_s value of 5.0 \AA smaller than ca. 7.3 \AA , expansion to the direction along the column axis might take place on polymerization in the crystals, resulting in amorphous polymer. On the other hand, **1e-B** has a d_s value of 7.4 \AA and is expected to polymerize topochemically to give a crystalline polymer. However, larger d_{cc} and/or two possible directions of polymerization led to amorphous polymers. These observations in quinodimethanes are quite similar to those of topochemical polymerizations in dienes for $d_s = 4.9\text{--}5.2 \text{ \AA}$ ⁵ and trienes and triynes for $d_s = 7.3 \text{ \AA}$.⁴

Conclusion

Novel highly conjugated monomers, 7,7,8,8-tetrakis(alkoxycarbonyl)quinodimethanes with methoxy (**1a**), ethoxy (**1b**), isopropoxy (**1c**), benzyloxy (**1d**), chloroethoxy (**1e**), and bromoethoxy (**1f**) as alkoxy groups, were synthesized, and their polymerizations in the crystalline state were investigated. Some of **1a-f** afforded two crystal forms depending upon recrystallization conditions, and their crystal structures were determined by X-ray crystallography. It was found that topochemical polymerizations of the quinodimethane monomers might take place when they are packed in the crystals with parameters of $\theta_1 = 30\text{--}33^\circ$, $\theta_2 = 83\text{--}89^\circ$, $d_s = 7.0\text{--}7.6 \text{ \AA}$, and $d_{cc} = 3.8\text{--}4.2 \text{ \AA}$.

Supporting Information Available: Experimental procedures, spectroscopic and analytical data, and X-ray crystallographic data in CIF format for 7,7,8,8-tetrakis(alkoxycarbonyl)quinodimethanes (**1a-f**). This material is available free of charge via the Internet at <http://pubs.acs.org>.

JA0386086